DES SIMULATION OF A FINITE CYLINDER MOUNTED ON A FLAT PLATE

Luciano G. Noleto
Universidade de Brasília. Departamento de Engenharia Mecânica, LEA - Laboratório de Energia e Ambiente. 70910-900 Brasília. DF. Brazil.
lucianonoleto@unb.br

Antonio C. P. Brasil Junior
Universidade de Brasília. Departamento de Engenharia Mecânica, LEA - Laboratório de Energia e Ambiente. 70910-900 Brasília. DF. Brazil.
brasiljr@unb.br

Abstract. *This paper aims to perform a numerical study of a structure represented by a cylinder mounted in a flat plate. The effect of the unsolved obstacles on the flow implies in a distributed mean momentum sink, and it demands additional terms in the transport equations for the turbulent quantities. The modeling of macroscopic behavior of this complex flow involves the averaged procedures and descriptions of composites flow. The simulation of the flow through a cylindrical obstacle will be done here to observe vortex formations for this flow. The simulation will be conducted using unstructured grids and Detached Eddy Simulation turbulence model (implemented in the CFX commercial software). The DES model is a hybrid formulation which allows a LES/URANS simulation simultaneously.*

Keywords: *DES model, Finite Cylinder, Vortex formation*

1. Introduction

The flow around a circular cylinder has several applications. One of them is at canopy flows, where the cylinder can represent an obstacle, being this obstacle one or several trees in a forest or buildings in a major city. The flow pattern is a horseshoe vortex close to the wall that the cylinder is mounted, and depending of the flow characteristics, a vortex shedding is developed downstream, with a 3-Dimensional separated flow at the free end surface. This separated flow has a major influence over the wake flow. The circular cylinder can be represented by a bluff body that shows 3-Dimensional altered flow characteristics in the axial direction. It is caused by the non-uniformity of free stream flow, longitudinal vortices and low aspect ratio of the cylinder (height is close to equal, or equal, to the diameter). The fact of the cylinder being finite influences the topology of the flow. The DES model is a good alternative for this flow. The DES model was proposed by Spalart (Spalart, 2000), and it means the ultimate hybridization of a LES approach. The DES principle lies on blending Large Eddy Simulation (LES) with Unsteady Reynolds Averaged Navier-Stokes (URANS) where, the flow receives two distinct approaches in different regions of the flow. At the region where the boundary layer is not separated,a RANS model. At the region where the boundary layer is already separated, the simulation is made using LES.

DES was tested in several cases of Large Eddy Simulation (LES), to check the reliability of the model for engineering cases. Like the work (Constantinescu and Squires, 2003) who investigate the flow over a sphere in super critical regime with LES and DES, concluding that the DES model accurately predict massively separated flows and it was able to predict also the large scale shedding of hairpin-like structures and the formation of Kelvin-Helmholtz instabilities. Other work (Squires et al., 2002), made a analysis of massive separated flows in aircrafts using DES, concluding that the prediction of lift and drag are accurate in comparison with flight data, and also predicts with accuracy the pressure in the supersonic flow over the aircraft. A recent work (Forsythe et al., 2001) used the DES model to predict the flow over a forebody cross section, concluding that the predictions of the model are robust, with little differences between experimental data and the simulation. Other recent work (Morton et al., 2002) make a assessment of unstructured grids in some cases, concluding that the use of that kind of mesh is easier to refine on complex geometries, and it consequence is more turbulent flow structures are resolved. A work made recently (Schimidt and Thiele, 2003) had simulated the flow around a aerospatiale A-airfoil with DES, and its results are reasonable if compared with LES. A work using DES and the circular cylinder (Travin et al., 2003) had shown good results for shedding frequencies.

Concerning to finite cylinder flows, there is the confirmation of the presence of a pair of vortices around the free end surface from iso-velocity lines in the wake near the tip region and this work identified this pair of vortices as trailing side tip vortices (Kawamura et al., 1984). There is also a work (Baban et al., 1989) who observed an increase in drag force fluctuations due to highly turbulent recirculation flow in the wake region, especially in the shear layer separated from the end of the cylinder. A visualization of the flow over the free end surface of a finite cylinder mounted on a flat plate using oil-streak line methods and smoke-laser (Roh and Park, 2003) showed that the flow at the free end surface is topologically characterized by two spiral nodes and a separation saddle point in the front portion and two attachment nodes and a separation saddle point in the rear part. A study of the free end effects in finite cylinder flows (Park and

Lee, 2000) observed that the vortex shedding frequency decreases and the the vortex formation region increases as the aspect ratio decreases. The vortex formation region and periodic vortex shedding disappear very close to the free end. A experimental study of a small forest model based on a single cylinder and a cylinder matrix (Cala, 1996) in wind tunnel obtained profiles who had shown great resemblance with similar work.

This paper will show results of the numerical simulation of a circular cylinder mounted in a flat plate with ANSYS-CFX commercial software and the DES SST model. The chosen case is the single cylinder studied by Cala (Cala, 1996).

2. Mathematical Modeling

2.1 Governing Equations

In a frame work for turbulence modeling, for incompressible turbulent flows, the conservation of mass, and momentum can be expressed by the classical Reynolds averaged equations given by:

$$\frac{\partial u_i}{\partial x_i} = 0 \tag{1}$$

$$\rho\left(\frac{\partial u_i}{\partial t} + u_j\frac{\partial u_i}{\partial x_j}\right) = -\frac{\partial p}{\partial x_i} + \frac{\partial}{\partial x_i}\left[(\mu+\mu_t)\frac{\partial u_i}{\partial x_j}\right] \tag{2}$$

In those equations u_i and p are the mean velocity and pressure fields and μ_t is the eddy viscosity, modeling in the framework of $k-\omega$ model as:

$$\mu_t = \rho\frac{k}{\omega} \tag{3}$$

Here, k and ω are the turbulent kinetic energy and eddy frequency.

2.2 The SST Model

Menter (Menter and Kuntz, 2003) created the SST model, and its principle lies on blending the $k-\epsilon$ and the $k-\omega$ model. Far from the wall, the model uses the $k-\epsilon$ formulation, and near the wall, the model uses the $k-\omega$ model. The transport equations are:

$$\rho\left(\frac{\partial k}{\partial t} + u_i\frac{\partial k}{\partial x_i}\right) = P_k - \beta' k\omega\rho + \frac{\partial}{\partial x_i}\left[(\mu+\frac{\mu_t}{\sigma_k})\frac{\partial k}{\partial x_i}\right] \tag{4}$$

$$\rho\left(\frac{\partial \omega}{\partial t} + u_i\frac{\partial \omega}{\partial x_i}\right) = \alpha\rho S^2 + \beta\rho\omega + \frac{\partial}{\partial x_i}\left[(\mu+\frac{\mu_t}{\sigma_\omega})\frac{\partial \omega}{\partial x_i}\right] + 2(1-F_1)\rho\sigma_{\omega 2} + \frac{1}{\omega}\frac{\partial k}{\partial x_i}\frac{\partial \omega}{\partial x_i} \tag{5}$$

The turbulent eddy viscosity is defined by:

$$\nu_t = \frac{a_1 k}{\max(a_1\omega, SF_2)} \tag{6}$$

S is an invariant measure of the tensor rate and F_2 is one of two blending functions of the model. The formulation of the blending Functions F_1 and F_2 are based on the distance of proximity of the surface and on the flow's variables. The Blending Functions F_1 and F_2 are given as follows:

$$F_1 = \tanh(\arg_1^4) \tag{7}$$

$$\arg_1 = \min\left[\max\left(\frac{\sqrt{k}}{\beta'\omega}, \frac{500\nu}{y^2\omega}\right), \frac{4\rho\sigma_{\omega 2}k}{CD_{k\omega}y^2}\right] \tag{8}$$

$$CD_{k\omega} = \max(2\rho\sigma_{\omega 2}\frac{1}{\omega}\nabla k\nabla\omega, 1, 0.10^{-10}) \tag{9}$$

Here, y is the distance to the wall. F_1 is equal to zero away from the surface ($k-\epsilon$ model), and switches over to 1 inside the boundary layer ($k-\omega$ model). F_2 is given by:

$$F_2 = \tanh(\arg_2^2) \tag{10}$$

$$arg_2 = \max\left(\frac{2\sqrt{k}}{\beta'\omega y}, \frac{500\nu}{y^2\omega}\right) \tag{11}$$

F_2 restrains the limitator for the boundary layer wall. A production limiter is used to avoid the growth of turbulence in stagnation regions:

$$P_k = \mu_t \frac{\partial U_i}{\partial x_j}\left(\frac{\partial U_i}{\partial x_j} + \frac{\partial U_j}{\partial x_i}\right) \tag{12}$$

$$\widetilde{P_k} = max(P_k, 10 \cdot \rho\beta^* k\omega) \tag{13}$$

The model's constants are accounted by a blend of the corresponding constants of the $k-\epsilon$ and $k-\omega$ models with the following function:

$$\alpha = \alpha_1 F + \alpha_2(1-F) + ... \tag{14}$$

The constants are β'=0.09, α_1=5/9, β_1=3/40, σ_{k1}=0.5, $\sigma_{\omega 1}$=0.5, α_2=0.44, β_2=0.0828, σ_{k2}=1, $\sigma_{\omega 2}$=0.856. The analytical expression for ω provided by ω-equation turbulence models allows a near-wall formulation, which gradually switches from wall-functions to low-Re near wall formulations. At the same time, the mesh is refined in wall normal direction.

2.3 The DES Model

As it said before, the DES model means a hybridization of a LES approach. Both of those approaches have its limitations. The RANS approach is limited to predict the separated flow, and LES has the difficulty in prepare the subgrid modeling to predict the non-separated boundary layer. DES takes advantage of the RANS method where the mean flow remains attached and steady while offering, like LES, the sensitivity to capture, for instance, wakes or recirculation zones. There are two issues in this approach:

- How fast the turbulent structures will develop after the formulation change to RANS from LES?
- How the changing formulation mechanism must be modeled, in order to avoid a grid induced separation?

The answer lies in the blending functions of the SST model. These functions will "shield" the boundary layer and minimize the grid-induced separation. As the SST model is based on a zonal formulation, differentiating the boundary layer of the rest of the flow, the blending functions of the model can also be used to formulate a zonal DES limiter. The formulation change will happen when the turbulent length scale obtained in the RANS section of the model surpasses the local grid spacing. The modeling of the DES SST model uses the SST model and the switching modeling, given as follows:

$$\varepsilon = k\beta'\omega = \frac{k^{\frac{3}{2}}}{L_t} \Rightarrow \frac{k^{\frac{3}{2}}}{C_{DES}\Delta} \tag{15}$$

For $C_{DES}\Delta < L_t$:

$$\Delta = max(\Delta_i); L_t = \frac{\sqrt{k}}{\beta'\omega} \tag{16}$$

Here, the switch from the SST model to an LES model is made only in regions where the turbulent length, L_t, predicted by the RANS model is larger than the local grid spacing. Far from walls, the length scale is redefined, increasing the magnitude of the destruction term in the turbulent kinetic energy equation, drawing down the eddy viscosity and allowing instabilities to develop, creating a cascade down to the grid scale as in classical LES. The model constant C_{DES} is of the order of one and it should be set so as the spectrum at high frequencies does not exhibit oscillations, and for the flow eddies, are not under-resolved at these frequencies. The length scale used in the computation of the dissipation rate in the equation for the turbulent kinetic energy is replaced by the local grid spacing Δ. The reason for choosing the maximum edge length in the DES formulation is that the model should return the RANS formulation in attached boundary layers. The maximum edge length is therefore the safest estimate to ensure that demand. Strelets (Strelets, 2001) propose the following modification to the model, formulated as a multiplier of the destruction term in the turbulent kinetic energy:

$$\varepsilon = k\beta'\omega \Rightarrow k\beta'\omega F_{DES}; F_{DES} = max(\frac{L_t}{C_{DES}\Delta}, 1) \tag{17}$$

Here, $C_{DES} = 0,61$ is the limiter who should be active in the RANS region, specifically in the $k-\epsilon$ region. The numerical formulation is also switched from an upwind biased in the RANS region and a central difference scheme in the DES region. The third blending function is modeled in CFX as follows:

$$F_{DES-SST} = max(\frac{L_t}{C_{DES}\Delta}(1-F_{SST}), 1) \tag{18}$$

Putting $F_{SST} = 0$ recovers the Strelets formulation. F_2, showed before, shields more of the boundary layer and is therefore the desired default. However, even F_2 does eliminate the problem, but reduces it by an order of magnitude. Since this model has a LES approach, the case needs a transient formulation. The set-up of the DES SST model was set according with the work of (Menter and Kuntz, 2003).

3. Computational Details and Boundary Conditions

For inflow surfaces the values of velocity, kinetic energy of turbulence and dissipation fields are prescribed. For outflow boundaries, the homogeneous Neumann conditions are prescribed for the same variables and the homogeneous Dirichlet boundary condition is used for the pressure field.

The single cylinder case studied by Cala (Cala, 1996) is a cylinder without pendulum movement, attached to the lower wall. For this case, experimental results of transversal and vertical velocity and respective fluctuations are available. Here, the cylinder has 75 mm of height and diameter of 19 mm. The inlet Reynolds number is set to the valor of 21000. Figure 1 shows the unstructured mesh used. There is a refinement at the surroundings of the cylinder and downstream of the domain. The CFX's inflation boundary resource is used to improve results near the cylinder. Here, the mesh has 97813 nodes, 538989 elements and 3960 prismatic elements. The transient simulation has a time step of 10^{-4} seconds with a total time of 100 seconds. The convergence criterion is set as 10^{-4} in RMS value of all fields norm.

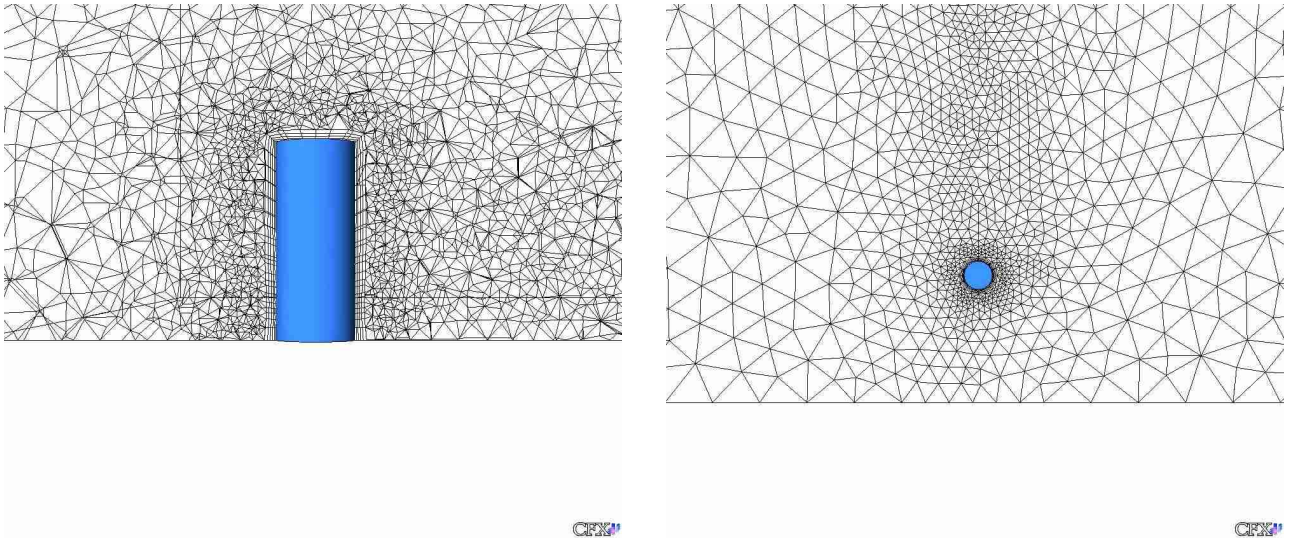

Figure 1. Cylinder mesh

4. Results and Discussion

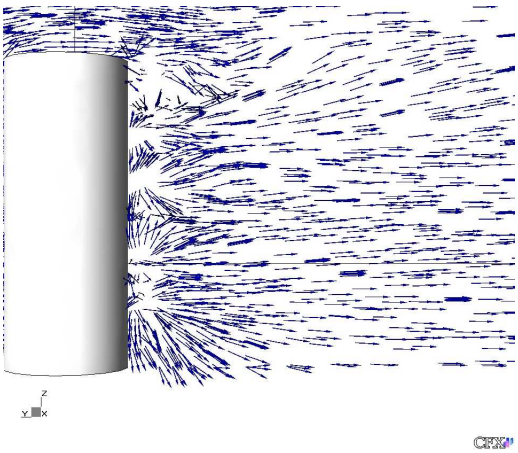

Figure 2. Velocity vectors

The presented results in streamlines and velocity vectors had shown the hydro dynamical characteristics of this kind of flow. The streamlines show that the turbulent wake has the natural complexity of that flow. The flow over a mounted

cylinder is very unique, because the flow topology has a behavior at the wake that is very controversial. A lot of open issues are shown at the literature. The boundary layer over the finite cylinder is far more complex than the 2-Dimensional infinite cylinder. At the 2-Dimensional case, there is a vortex shedding which happens in a characteristic frequency. The length scale varies proportionally with $l^{1/2}$. For the finite cylinder case, the wake topology stands in the way of vortex shedding. Figures 3 and Figure 2 show the beginning of the formation of horseshoe vortex and the separation of the flow at the top of the cylinder, which resembles the work of Roh (Roh and Park, 2003). But this kind of vorticity appears close to the ground, which was not observed here. The horseshoe vortex near the ground is generated from the junction of the cylinder with the plate. The formed horseshoe vortex has its effects limited to the region near the wall. The experimental result of Cala (Cala, 1996) show, near the plate, a peak of the velocity fluctuation spectra. This indicates a vortex shedding at that specific point, with a characteristic frequency. At the top of the cylinder, the flow presents itself as 3-Dimensional and unorganized. The appearance of vortex shedding and Von Kárman wakes is governed by the aspect ratio of the cylinder. Eventually, this kind of vorticity appears at the bottom of the cylinder. The flow moves upward and accelerates near the free end, to separate from the cylinder circumference at the free end. At the central wake, the separated shear layer is declined, showing the same effect observed by Park (Park and Lee, 2000).

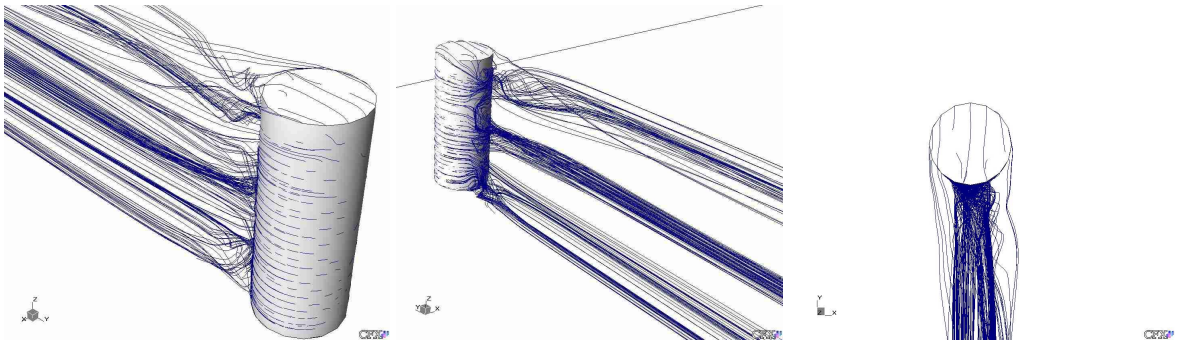

Figure 3. Streamline Display

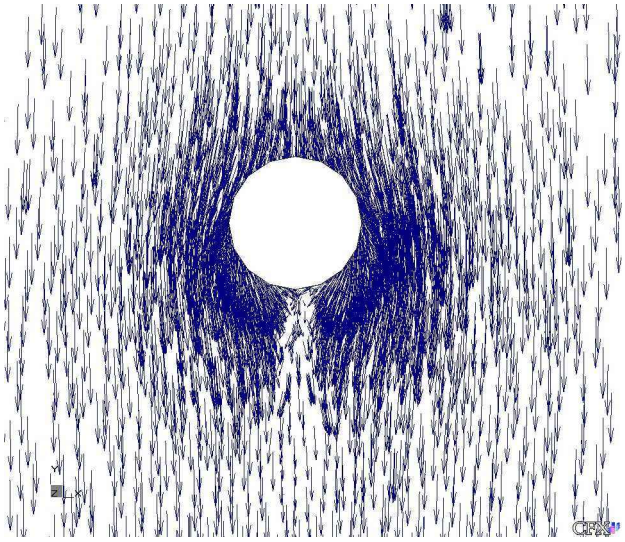

Figure 4. Velocity vectors - 3,75 mm

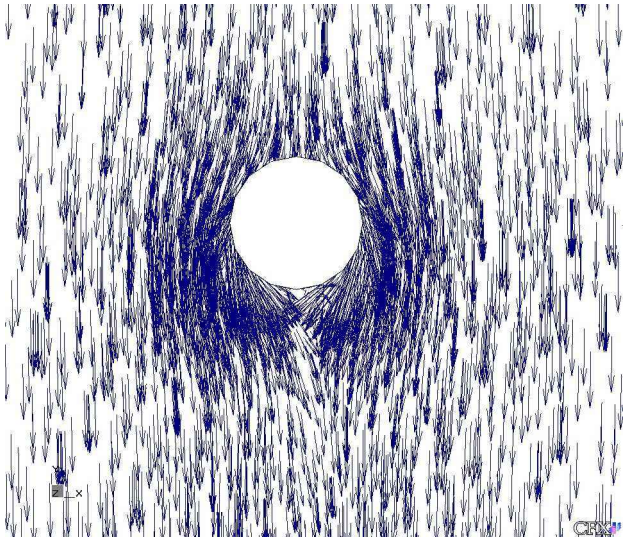

Figure 5. Velocity vectors - 33,75 mm

The results in figures 4, 5, 6 and 7 show the velocity vectors for 4 aspect ratios. The 2 first aspect ratios were taken at the bottom of the cylinder. Here, there is the beginning of the formation of clockwise and counterclockwise rotating vortices. Those vortices are similar to the vortices formed at the leading edge of a delta wing. At 33,75 mm the rotating vortices start to show a definite form. At that location, those vortices are slight asymmetric, which show the beginning of a vortex shedding, which concurs with the experimental result of Cala (Cala, 1996). For low values of velocity near the plate, the ascending flow is inhibited, which give rise to the turbulence at that region, aided by shear. Near to the top of the cylinder, those vortices begin to form and have definite forms. According to Park (Park and Lee, 2000), they are formed by the roll-up motion of the shear flow separated from the edges of the near end of the cylinder. This shear flow descends along the central region of the wake. At the top of the cylinder, the result is visibly asymmetric, showing tornado-like vortices rooted at the surface, which is confirmed by the streamline display. This result shows agreement with the results of Roh (Roh and Park, 2003) and Kawamura (Kawamura et al., 1984). They visualized the existence of a pair of swirl-like

flow at the free end surface, which is also observed by the streamline display. The overall vortex topology at the top of the cylinder is tornado-like vortices, with counter rotating vortices.

The graphical analysis show that the similar behavior of the profiles downstream of the flow is not observed to regions close to the cylinder in the transversal and vertical profiles (Figures 8 to 13). At 2D, the profile has a different pattern if compared with the other profiles. The 3-Dimensional structure of the flow induces a growth of the velocity close to its symmetry line. This behavior was observed by Cala (Cala, 1996), and he interpreted it as a recuperation of the velocity behind the recirculation zone. The numerical results of transversal profiles had shown resemblance with the experimental results, with minor differences between the experimental and the numerical results. At the transversal profile located in 2D, the numerical result has predicted the peak at the fluctuation profile, observed at 1,5R, differently than the experimental results. According to Cala, this is the limit where the vortex structure produces an important generation rate of turbulent kinetic energy. The vertical profiles show the wake form, which shows the recuperation of the kinetic energy downstream. Slowly, the level of turbulent intensity diminishes downstream. The numerical results here, with slight differences, show good resemblance with experimental data as well.

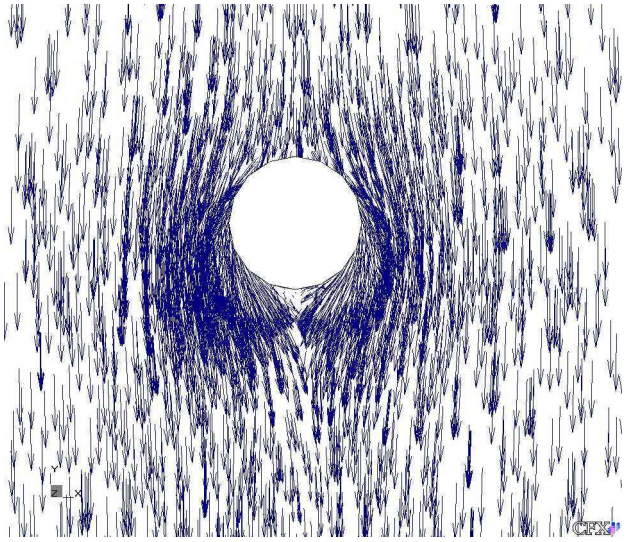

Figure 6. Velocity vectors - 41,25 mm

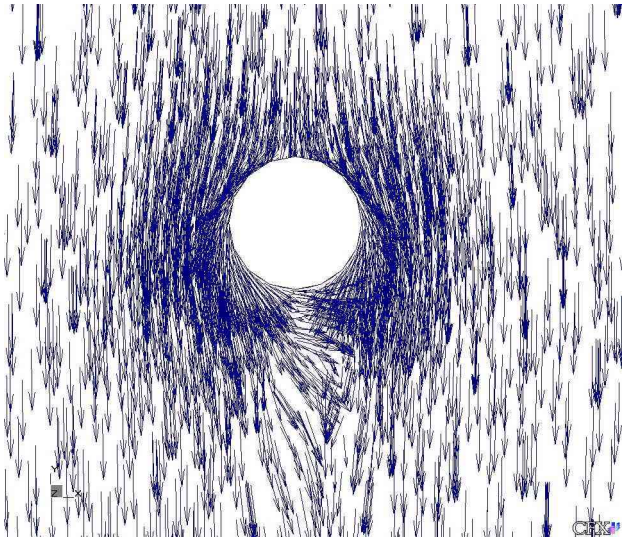

Figure 7. Velocity vectors - 65,25 mm

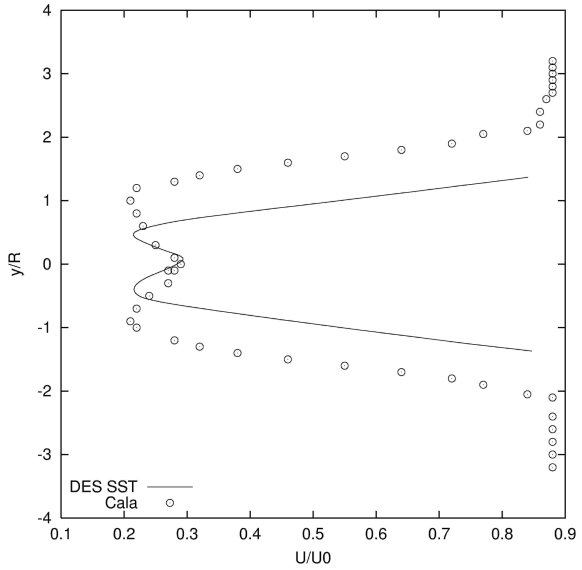

Figure 8. X=2D - Transversal Profile

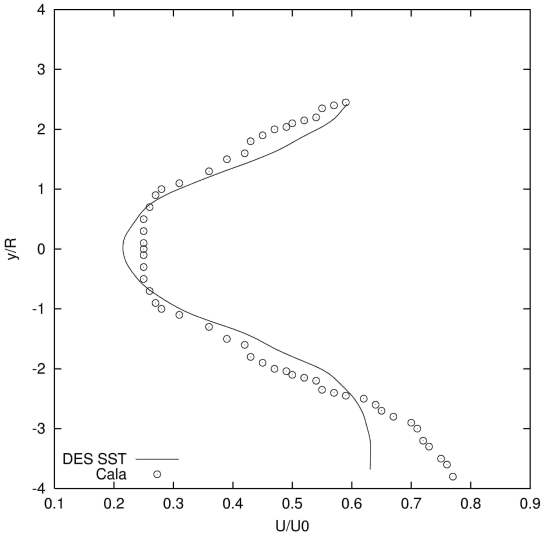

Figure 9. X=4D - Transversal Profile

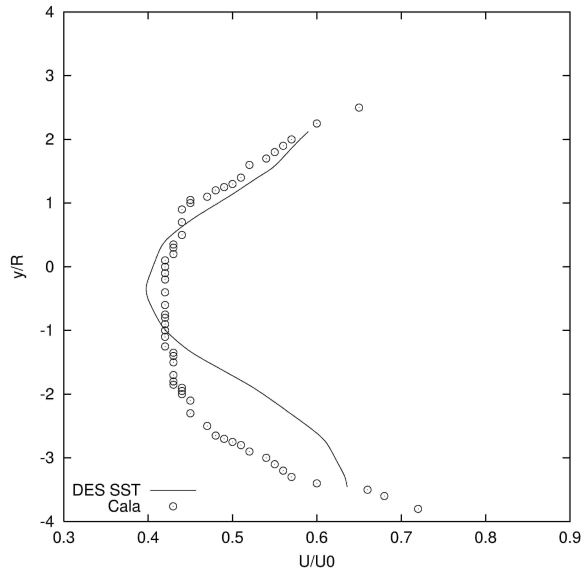

Figure 10. X=6D - Transversal Profile

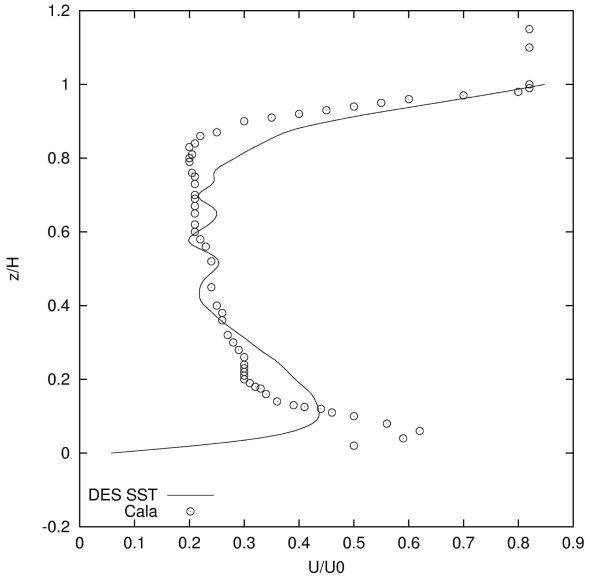

Figure 11. X=2D - Vertical Profile

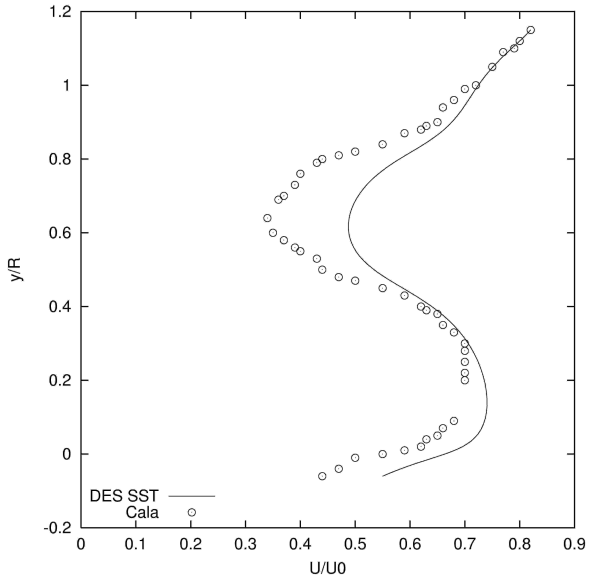

Figure 12. X=4D - Vertical Profile

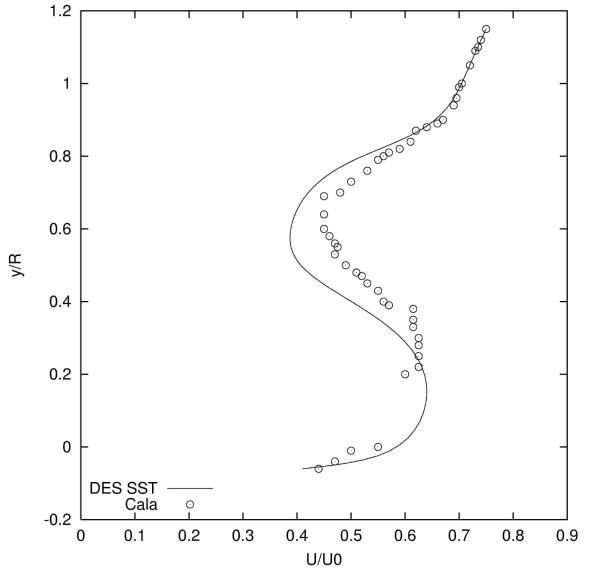

Figure 13. X=6D - Vertical Profile

5. Conclusion

Results of a numerical simulation over a finite cylinder mounted at a flat plate were made. The results are showed at velocity vectors, streamlines and graphical validation, where the numerical data is compared to experimental data.

The velocity vectors and streamline display show the beginning of the formation of horseshoe vortex, which holds some agreement with the experimental result. There is also the separation of the flow at the top of the cylinder, which agrees too with experimental results. The visualized result at the top of the cylinder shows a swirl-like flow, with tornado-like flow. The velocity vectors displayed at several aspect rates of the cylinder show the beginning of the formation of counter-rotating vortex and, at the top, the asymmetric vorticity shows the tornado-like vortices. The graphical analysis shows that the numerical results have resemblance with experimental result, but some profiles have slight differences if compared with experimentation.

Concluding, the DES model shows itself as a good model to simulate open cases, which was observed at the literature and confirmed here. For this case the model must be compared with other numerical results, made by RANS and LES models separated. That way, the model can have the proper discussion about its efficiency.

6. References

Baban, F., So, R., and Otugen, M., 1989, Unsteady Forces on circular cylinders in a cross-flow, "Experiments in Fluids", Vol. 7, pp. 293–302.

Cala, C. E. C., 1996, Estudo do Escoamento Turbulento Dentro e Sobre uma Matriz de Cilindros Pendulares, Master's thesis, Universidade de Brasília.

Constantinescu, G. S. and Squires, K. D., 2003, LES and DES Investigations of Turbulent Flow over a Sphere at Re=10,000, "Flow, Turbulence and Combustion", Vol. 70, pp. 267–298.

Forsythe, J. R., Squires, K. D., and Spalart, P. R., 2001, Detached Eddy Simulation of the Separated Flow over a Forebody Cross Section, B. J. Geurtz, R. F. and Metais, O., editors, "Direct and Large Eddy Simulation IV", Vol. 8 of "ERCOFTAC Series", pp. 481–500.

Kawamura, T., Hiwada, M., Hibino, T., Mabuchi, I., and Kumada, M., 1984, Flow around a finite circular cylinder on a flat plate, "Bull JSME 27:2142-2151".

Menter, F. R. and Kuntz, M., 2003, Development and application of a zonal DES turbulence model for CFX 5, Ansys cfx validation report.

Morton, S., Forsythe, J., Squires, K., and Wurtzler, K., 2002, Assessment of unstructured grids for Detached-Eddy Simulation of high Reynolds number separated flows, "Proceedings of the Eighth International Conference on Numerical Grid Generation in Computational Field Simulations".

Park, C. and Lee, S., 2000, Free end effects on the near wake flow structure behind a finite circular cylinder, "Journal of Wind Engineering and Industrial Aerodynamics", Vol. 88, pp. 231–246.

Roh, S. and Park, S., 2003, Vortical flow over the free end surface of a finite circular cylinder mounted on a flat plate, "Experiments in Fluids", Vol. 34, pp. 63–67.

Schimidt, S. and Thiele, F., 2003, Detached Eddy Simulation of Flow around A-Airfoil, "Flow, Turbulence and Combustion", Vol. 71, pp. 261–278.

Spalart, P. R., 2000, Strategies for Turbulence Modelling and Simulation, "International Journal of Heat and Fluid Flow", Vol. 21, pp. 252–263.

Squires, K. D., Forsythe, J. R., Morton, S. A., Strang, W. Z., Wurtzler, K. E., Tomaro, R. F., Grismer, M. J., and Spalart, P. R., January 2002, Progress of Detached Eddy Simulation of Massively Separated Flows, "AIAA 2002-1021".

Strelets, M., 2001, Detached Eddy Simulation of massively Separated Flows, "AIAA 2001-0879".

Travin, A., Shur, M., Strelets, M., and Spalart, P., 2003, Detached Eddy Simulation Past a Circular Cylinder, "Flow, Turbulence and Combustion", Vol. 70, pp. 293–313.